3D- Finite Element Model for GaAs α-particles pixel detector

MARIA RIZZI, MICHELE MAURANTONIO, BENIAMINO CASTAGNOLO

Dipartimento di Elettrotecnica ed Elettronica,
Politecnico di Bari
v. E. Orabona, 4 - 70125 Bari
ITALY

Abstract: In this paper a numerical study of the GaAs pixel detector performance is presented. The model is based on the 3D-Finite Element Method (FEM) and takes into account the carriers trapping and emission phenomena. The numerical simulations obtained, confirms the electrical behaviour of pixels and permits the indirect evaluation of the charge collection efficiency through a preliminary determination of the real trap distribution and transport parameters depending on the electric field.

Key words: X-ray detector, Schottky diode, pixel matrix

1 Introduction

Digital radiography is an imaging modality that uses electronics and computational techniques [1]. Amongst the materials suitable to be used as detectors, semiconductors seem to be the best choice [2]. While silicon is almost a perfect material for particle physics detectors, allowing the shaping of electric fields by tailored impurity doping, the need of high photon absorption efficiency in radiological applications requires the study and use of semiconductor materials with high atomic charge, such as GaAs. In fact the GaAs wide bandgap (1.43eV), the high atomic number and the well-established microelectronics technology are good preliminary conditions for developing room temperature X-ray detectors with high energy resolution and high efficiency up to 100 keV [3], [4], [5], [6], [7], [8].

Devices in GaAs contain a high concentration of traps, which decreases the charge collection efficiency of such detectors: traps influence the detector performance by means of carrier capture and electric field spatial distribution change. In order to relate the trap characteristics to the detector behavior, in this paper a numerical model of the induced current signal has been devised. The analysis is carried out adopting the 3D- Finite Element method (FEM) and takes into account trapping and generated carriers phenomena.

In section 2 the GaAs detection property and some fabrication options are indicated. Section 3, the principles of the method and the new model are presented. In section 4 the model is validated through the comparison with experimental data. Moreover, some conclusions are drawn out.

2 Semiconductor detection property

Interaction between radiation and a suitable material generates electrical charges (photoelectric effect), detected by means of the application of an electric field.

Gases, cryogenic liquids and semiconductors are the most used materials. Due to the lower energy necessary to produce an electron-hole pair (3-6eV vs. 30eV necessary to free an electron in gas detectors), it is possible to produce a higher charge adopting semiconductor detectors with the same energy amount. Therefore, the input signal to noise ratio is higher and, consequently, the detector front-end simpler. Moreover, material with high atomic mass have high X-ray sensitivity. In fact, the probability of interaction between an X-ray beam and a material having atomic number Z is proportional to Z^n ($4<n<5$).

Due to the high efficiency, high spatial and energetic resolution expected using digital detectors, semiconductors seem to be the best choice for these applications. Amongst the commercially available ones, the GaAs semiconductor family is one of the most suitable for radiological digital application.

The GaAs high resistivity, for its high-energy bandgap (1.43eV at room temperature), reduces leakage currents. Moreover the high atomic number improves the photoelectric interaction.

The previous features, together with the high electron mobility, allow a decrease in the

exposure time of the radiographed object, which determines a reduction of the radiation amount. This characteristic is very important, especially in medical applications.
For what the architecture is concerned, the need of an intrinsic, direct relation between the detector architecture and the radiographic image, makes the pixel-matrix architecture the best choice.
A read-out section is employed for collecting and transmitting data.
The advances in microelectronic technology make it possible to integrate the front-end electronic directly below each pixel.
The whole read electronic section, connected to each pixel, is integrated on a GaAs area having dimensions equal to that of the pixel.

3 Principles of the method and Mathematical model

To link the characteristics of the pixel with the device performance, a 3D-numerical model of the photoeffect-generated current has been studied. The model adopts the finite element analysis and it is implemented in Matlab R14 environment. A variable step mesh has been created to solve the discrete Laplace equation by using an iterative method.
The model evaluates the current signal induced by the motion of the single photogenerated carrier by the Ramo's theorem [9], [10].
When a carrier pair is generated in a given position, the charge induced on the collecting electrode is calculated taking into account the contribution of both electrons and holes. If trapping occurs, an incomplete charge collection is observed. The Shockley Read Hall (SRH) recombination theory is considered as base model for the carriers trapping and generation phenomena.
The carrier trapping is described by means of two characteristic times: the mean trapping time of electrons and that of holes. Trapping of a carrier occurs when its trapping time is shorter than the transit time. Also the detrapping mechanism is taken into account in this model [11,12,13,14].
Normally the collected charge efficiency, which is an integral parameter, is used in order to determine the total amount of collected charge. But in this model the efficiency is substituted by the determination, point by point, of the net charge due to the carriers trapping and re-emission actions.
By iterating the mathematical process for every generation point, the evaluation of the overall collected charge is made possible.

The photons interaction point is generated considering the *heavy ion* effect (fig.1), able to reproduce the crossing of an alpha particle or of a heavy ion. When this crosses a device, it looses energy and creates a number of electron-hole pairs. These charges are collected by the electric field which is present in the component. Important factors are the energy and the type of the ion, the angle of penetration of the ion and the relation between the energy loss and the number of pairs created [15].

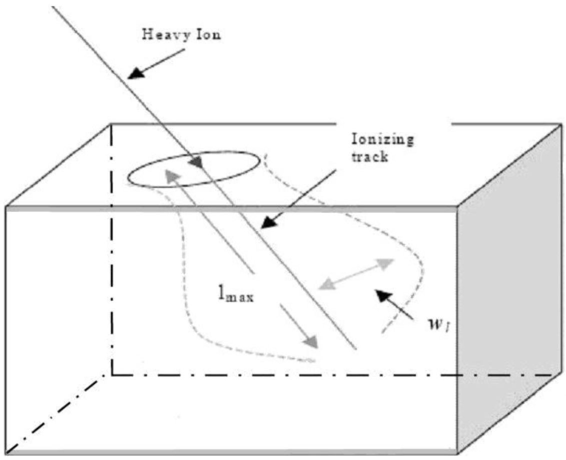

Fig 1 Heavy ion model

The generation rate caused by a heavy ion is computed by:

$$G(l,w,t) = LET(l) \times R(w) \times T(t) \quad (cm^{-3}s^{-1}) \qquad (1)$$

where *l* is the penetration length of the particle, *w* is the width of the generation cylinder and *t* is the time.
T(*t*) is defined as a gaussian function and is given by:

$$T(t) = \frac{2e^{-\left(\frac{t-time}{shi}\right)^2}}{shi\sqrt{\pi}\left(1-erf\left(\frac{time}{shi}\right)\right)} \qquad (2)$$

time (s) is the moment of the heavy ion penetration, *shi* (s) is the characteristic value (standard deviation) of the Gaussian.
LET(*l*) (cm^{-3}) is the linear energy transfer and is the fundamental parameter to define how many pairs/μm the heavy ion generates. Its expression is given by:

$$LET(l)=a_1+a_2 \times l + a_3\, e^{a_4 \times l}+k[c_1 \times (c_2+c_3 \times l)^{c_4} + Lef(l)]$$

where *Lef(l)* are additional arbitrary values and a_i and c_i are constant values, depending on the semiconductor properties.
R(*w*) is the distribution of the ionizing track on the plane transversal to the cross direction. The exponential case has been considered for our simulations. *R*(*w*) is given by:

$$R(w) = e^{-\left(\frac{w}{w_t}\right)} \qquad (3)$$

The current induced by the motion of a puntiform charge in a ionized medium between planar electrodes is, according to the Ramo's Theorem:

$$i(t) = q\frac{E(x,t)v_d(x,t)}{\psi(D)} \qquad (4)$$

where ψ is the electrostatic potential, v_d the drift velocity of the carrier, E the electric field intensity and D the distance between electrodes.
The charge induced in the external circuit are:

$$q_e = q\left[1 - \frac{\psi(x)}{\psi(D)}\right] \qquad (5)$$

$$q_h = q\frac{\psi(x)}{\psi(D)} \qquad (6)$$

where $\psi(x)$ is the potential at the position of the SRH center (P_0) .
Using a three-dimensional model and supposing that δn_0 electron/hole pairs are generated at initial time at a generic P_0 (x_0,y_0,z_0) point between the Schottky contacts, the charge induced by the motion of electrons and holes, before reaching the electrodes, is:

$$\Delta Q_{e/h}(t) = \pm\delta n_0(t)q\frac{(x(t) - x_0)}{D} \qquad (7)$$

where electrons are supposed to move along the positive x direction and holes in the opposite direction.
The dependence of δn_0 by t derives by the trapping actions which cause an exponential decay of free carriers as follows [12],[13]:

$$\delta n(t) = \delta n(0)e^{-\frac{t}{\tau_c}} \qquad (8)$$

where τ_c is the capture mean time.

Considering separately the effect of electrons and holes, the expression of the total charge induced is [16]:

$$\Delta Q^0{}_{tot} = \Delta Q^0{}_e + \Delta Q^0{}_h \qquad (9)$$

where:

$$\Delta Q^0{}_e = \frac{q}{D}\sum_{i=i_0}^{i_D}\delta N_0(t_i, x_i)\,\Delta x_i \qquad (10)$$

$$\Delta Q^0{}_h = \frac{q}{D}\sum_{i=0}^{i_0}\delta N_0(t_i, x_i)\,\Delta x_i \qquad (11)$$

The electron current signal at the i-th iteration step, can be approximated as follows:

$$I_e(t_i) = \frac{\Delta Q^0{}_e(t_i) - \Delta Q^0{}_e(t_{i-1})}{\Delta t_i} \qquad (12)$$

and a similar expression is valid for the hole current $I_h(t_i)$ deriving from eq. (11).
The same mathematical procedure can be iterated for every generation point. Therefore, it is possible to evaluate the overall collected charge by summing all the contributions from all the generation points.

4. Model Validation

The realized detector is a Schottky diode made on semi-insulating, Vertical Gradient Freeze (VGF), (100) oriented single crystals GaAs substrate, 200 µm thick. The substrate has the resistivity of $9.3\times10^7\Omega$cm, the mobility equal to $6944 cm^2V^{-1}s^{-1}$, the carriers concentration of 9.4×10^6 cm^{-3} and the Etch Pith Density (EPD crystal defect) of 1055 cm^{-2}.
Each pixel consists of two Schottky junctions, one of which polarized inversely. They are connected to an electronic front-end which provides for recording and amplifying signals. The Schottky contacts were realized on the front and on the back surfaces of the wafer with Ti/Pt/Au (30/30/60 nm) metalization process [17].
The detector has been modeled with a three-dimensional geometry (fig 2). For the model used in the experiment, each pixel is 200µm thick, 55µm wide and long.

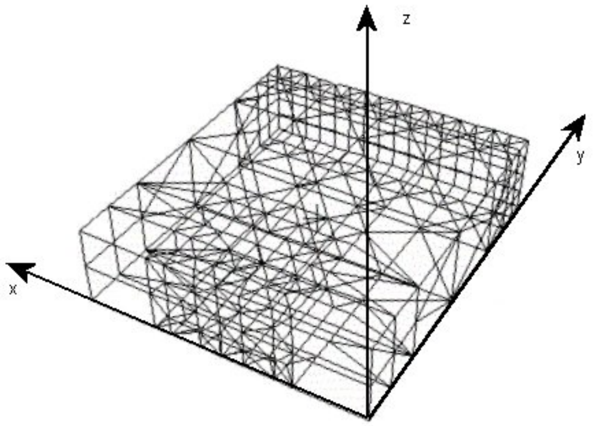

Fig. 2 Three-dimensional mesh adopted in the FEM simulation

To have a better performance in terms of charge collection, a guard-ring has been realized around each pixel of the detector. The guard-ring is 30μm thick and the distance between the guard-ring and the pixel is 5μm. The presence of guard-ring makes the electric field uniform and electrons move along fairly straight line, orthogonal to the contacts (fig.3-4).

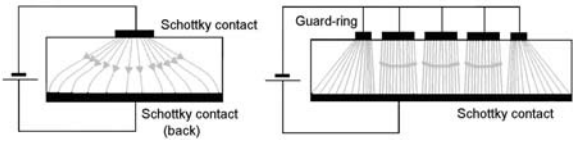

Fig.3 J flux lines distribution

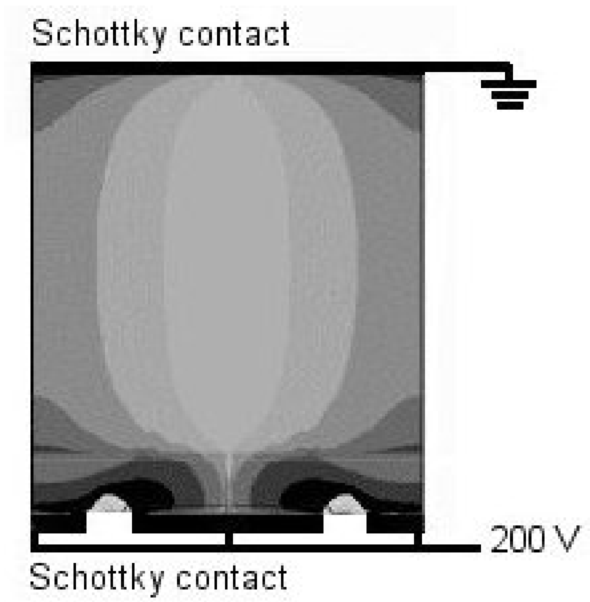

Fig.4 Simulation result of J flux lines distribution with guard-ring

The operating condition is obtained biasing the pixel in a range from 0 to 200V and irradiating it with 60KeV photons (simulating a ^{241}Am source) impinging on the back side Schottky contact.
To avoid leakage currents, a SiN dielectric layer (300 nm) is deposited on the wafer surface. The full depletion region is realized starting from 150 V.
In the simulation of the induced signal, two types of donor traps and of acceptor traps have been considered (tab.1). The spatial distribution of the electric field is obtained with the following set of parameters: electrode distance equal to 200μm, bias voltage equal to 200V, and a single couple electron/hole generation 25μm from the back side Schottky contact.

Trap	*Concentration (cm^{-3})*	*Capture cross section (cm^2)*	*Energy level (eV)*
E1	1.2×10^{15}	2.0×10^{-15}	0.560
E2	2.0×10^{16}	5.0×10^{-14}	0.790
H1	3.0×10^{15}	1.0×10^{-13}	0.410
H2	7.0×10^{14}	7.0×10^{-17}	0.510

Tab.1 Characteristics of electron (E_i) and hole (H_i) traps

Fig.5 shows the separation between the back side Schottky region and the active zone characterized by high field. The generated carrier spatial density decreases with the distance from the generation point: the electron capture increases dramatically after they reach the active region.
As the electron drift velocity is higher than that of the holes in the active region, the slope of the curve for electrons is greater with respect to the holes (fig.5).

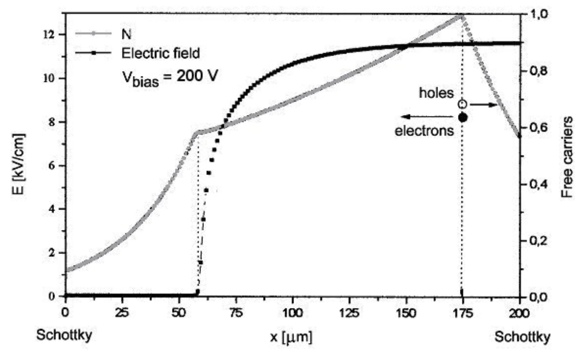

Fig. 5 Electric field distribution and generated carriers spatial density

In fig. 6 the shape of the J flux distribution is indicated in presence of a particle which hits to normally the pixel surface in the center (a) and in a point 3 μm distant far from the center (b).

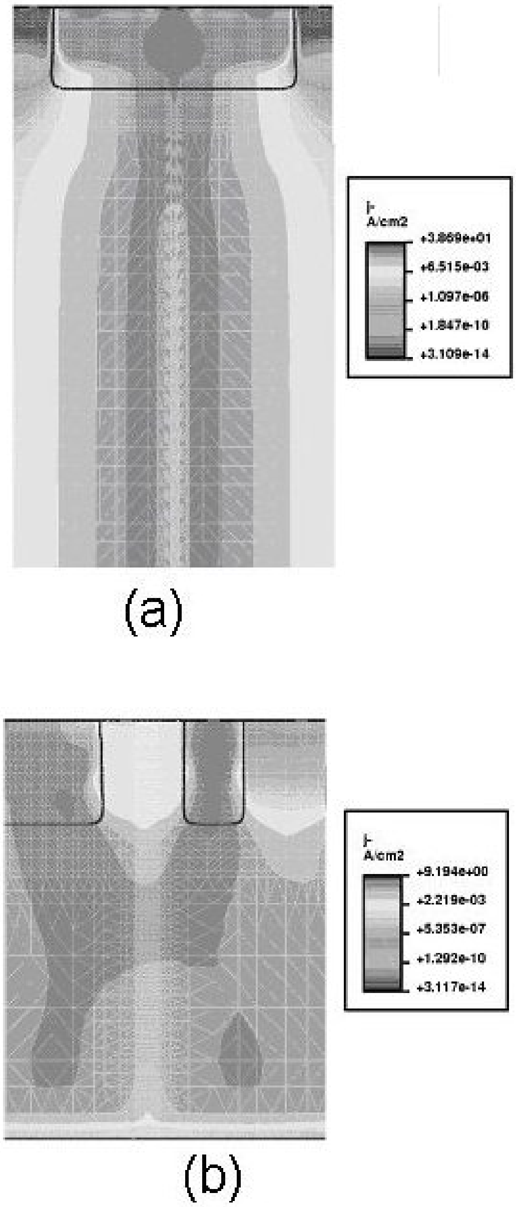

Fig. 6 J flux distribution for a collision normal to the center of the pixel surface (a) and in a point 3 μm distant (b)

To verify the 3D pixel model, the Charge Collection Efficiency (CCE) has been simulated and compared with the values obtained sperimentally. Indicating by H_0 the channel number corresponding to the maximum count number, the CCE is determined using the following expression:

$$CCE[\%] = \frac{H_0(GaAs)}{H_0(Si)} \frac{\varepsilon(GaAs)}{\varepsilon(Si)} 100 \qquad (13)$$

where ε(GaAs) = 4.3eV and ε(Si) = 3.6eV represent the average electron-hole generation energy.

In particular for this detector, a CCE value of about 90 - 95% is obtained for an electron/hole generation point 20 - 30 μm from the back side Schottky contact (fig. 7).
In fig. 8, the shape of the simulated and tested pixel I-V characteristic is indicated. It is shown the good accordance between the model simulation values and the experimental results

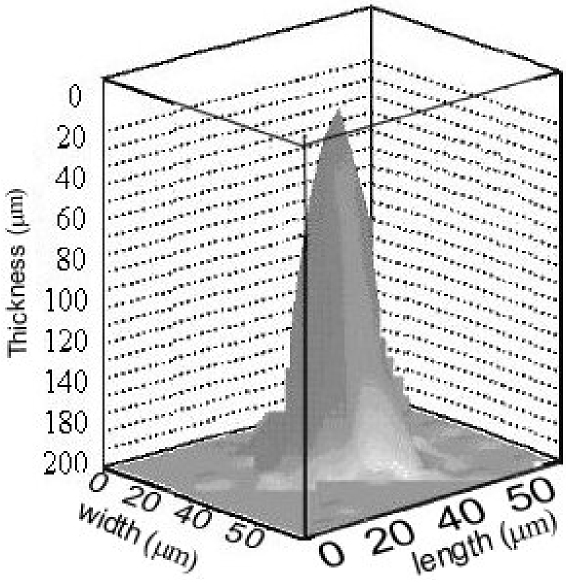

Fig. 7 Simulated 3D CCE values on a single pixel

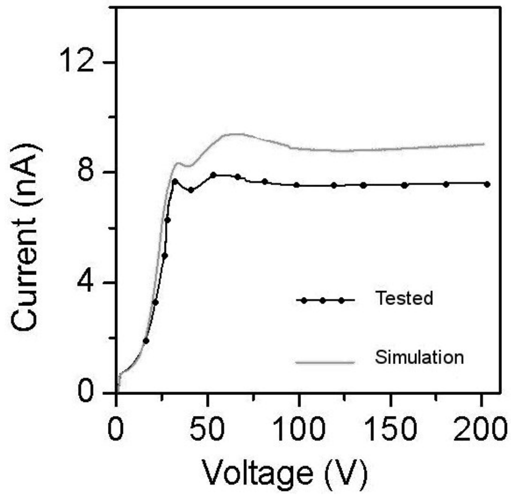

Fig. 8 Comparison between the tested and simulated values

5. Conclusions

In this paper a new model of a pixel matrix digital radiography system has been realized. The model performs a three-dimensional analysis adopting the Finite Element Method. The model takes into account both the hole/electron trapping and de-trapping mechanisms, implementing the SRH

regeneration equation, and both the carriers generation, considering the *heavy ion* effect.
Some different pixels have been realized and electrically tested. The experimental measures confirm the results of the proposed model.

References

[1] M. E. Fantacci "Pixels GaAs Detectors for Digital Radiography", *Proceedings of 3rd International Workshop on Gallium Arsenide and Related Components*, pp. 225-231, 1996

[2] W. Bencivelli, E. Bertolucci, U. Bottigli, A. Cola, M.E: Fantacci, P. Rizzo, V. Rosso, A. Stefanini, "Electrical Characterization and Detector Performances of a LPE GaAs Detector for X-Ray Digital Radiography", *Nuclear Instuments and Methods in Physics Research*, vol. A-346, pp. 372-378, 1994

[3] E. Vittone, C,. Manfredotti, F. Fizzotti, K, Mirri, E. Gargioni, P. Polesello, A. Lo Giudice, S. Galassini, F. Nava, P. Vanni, P. Rossi, "IBIC analysis of gallium arsenide Schottky diodes", *Nuclear Instuments and Methods in Physics Research*, vol. B-158, pp. 470-475, 1999

[4] D. R. Dance, "The Physics of Medical Imaging" pp. 27, *S. Webb editor*, 1990

[5] E. Bertolucci, "Digital Medical Imaging with GaAs Detectors", *Proceedings of 3rd International Workshop on Gallium Arsenide and Related Components*, pp. 211-216, 1996

[6] P. Randaccio "Evaluation of Elemental and Compound Semiconductor for X-Ray Digital Radiography", *Nuclear Instuments and Methods in Physics Research*, vol. A-310, pp. 210-214, 1991

[7] D.S. McGregor, G.F. Knoll, "Bulk GaAs Room Temperature Radiation Detectors" *Nuclear Instuments and Methods in Physics Research*, vol. A-322, pp. 487-492, 1996

[8] G Bertuccio, R. Casiragh, D. Maiocchi, A. Owens, M. Bavdaz, A. Peacock, H. Andersson, S. Nenonen "Noise analysis of gallium arsenide pixel X-ray detectors couplet to ultra-lownoise electronics" IEEE Trans. on Nuclear Science, vol. 50, n.3, pp.723-728, 2003

[9] P. De Visschere "The validity of Ramo's Theorem" Solid State Electronics, vol.4, pp.455-459, 1990

[10] H. Kim, H.S. MIN, W. Tang, Y.J. Park "An extended proof of the Ramo-Shockley theorem",Solid State Electronics, vol.34, pp.1251-1253, 1991

[11] D. S. McGregor, D. A. Rojeski, "Evidence for field enhanced electron capture by EL2 centers in semi-insulating GaAs and the effect on GaAs radiation detectors", Journal of Applied Physics, Vol. 75 N. 12, p. 7910 (1994).

[12] A.Cola, F.Quaranta, L.Vasanelli, C.Canali, A.Cavallini, F.Nava, and M.E.Fantacci, "A Study of the Trap Influence on the Performances of Semi-Insulating GaAs Pixel Detectors" *Nuclear Instruments and Methods in Physics Research,* pp. 395 349 (1997)

[13] A. Cola, F. Quaranta, M.A. Ciocci, M.E. Fantacci, "A Study of the Electrical and Charge Collection Properties of Semi-Insulating GaAs Detectors", *Nuclear Instruments and Methods*, Vol. A380, pp 66-69 (1996)

[14] S: P. Beaumont, F. Foster, G. Hughes, B. K. Jones, J. Santana I. J. Saunders, T. Sloan, "GaAs solid state detectors for particle physics", *Nuclear Instruments and Methods in Physics Research*, A322, 472-482, (1992)

[15] *J.S. Laird, T. Hirao, S. Onoda, H. Mori, H. Itoh* " Temperature dependence of heavy ion induced current transients in Si epilayer devices", *6th European Conference on Radiation and Its Effects on Components and Systems, 2001*. pp.125 - 131, 10-14 Sept. 2001

[16] M. Rizzi, V.Antonicelli, B. Castagnolo, "New model for a GaAs X-ray pixel detector" *IEE Proceedings on Circuits, Devices and Systems*, vol. 150 ,n. 3 , 6 pp. 210 – 216 (2003)

[17] B. L. Sharma "Metal-semiconductor Schottky barrir junction and their applications", 1994, *Plenium Press*,

Acknowledgement

The work is carried out under the financial support of the Ministero dell'Istruzione, dell'Università e della Ricerca Scientifica, in the frame of Cluster C26: "Modellazione, sperimentazione e diagnostica di strutture in materiali innovativi"